MIXING TRANSITION IN THE MAGNETIC RAYLEIGH-TAYLOR INSTABILITY

Antoine Briard,
CEA, DAM, DIF, 91297 Arpajon, France
antoine.briard@cea.fr

Benoît-Joseph Gréa
CEA, DAM, DIF, 91297 Arpajon, France
LMCE, Université Paris-Saclay, France,
benoit-joseph.grea@cea.fr

Florian Nguyen
CEA, DAM, DIF, 91297 Arpajon, France
florian-nguyen@orange.fr

ABSTRACT

The effect of a mean magnetic field on the development of the Rayleigh-Taylor instability is investigated using high-resolution direct numerical simulations. The magnetic field is applied and maintained perpendicular to the interface between two miscible fluids. It initially inhibits small-scale shear instabilities so that mixing is reduced, and hence structures are strongly stretched in the vertical direction and rapidly grow. At some point, when the typical vertical velocity exceeds the Alfvèn velocity imposed by the mean magnetic field, the flow experiences a rapid transition to turbulence, shear instabilities develop, structures break and mixing occurs.

INTRODUCTION

Perturbations at the interface between two fluids such that the direction of the acceleration is opposite to the mean density gradient may become unstable with the baroclinic production of vorticity: this is the Rayleigh-Taylor instability (RTI). In the case of miscible fluids, a turbulent mixing zone emerges and grows with time. If these two fluids have magnetic properties, the magnetohydrodynamics (MHD) equations are required, in addition of the Navier-Stokes equations, to describe the full dynamics. The magnetic Rayleigh-Taylor instability (MRTI) can play an important role in several astrophysical systems, such as for example the formation of the Crab nebula, the emergence of magnetic fluxes from the Sun interior, the accretion onto compact objects, the expansion of young supernova remnants, ... (see Carlyle & Hillier (2017); Hillier (2018) and references therein).

For inviscid and incompressible fluids with a mean magnetic field applied parallel to the interface, a perturbation of wavevector $\boldsymbol{k}$ parallel to the interface is unstable only if B_0 (the mean magnetic field intensity scaled as the Alfvèn velocity) is smaller than the critical value $B_c = \sqrt{\mathscr{A} g/k}$, where $\mathscr{A}$ is the Atwood number, $k = |\boldsymbol{k}|$ the wavenumber, and g the magnitude of the gravitationnal acceleration (Chandrasekhar (1961)). Early simulations have revealed that ascending and descending structures are greatly smoothed when $B_0 < B_c$, changing the usual picture of growing mushrooms into elongated fingers (Jun *et al.* (1995)). This observation was confirmed later in 3D direct numerical simulations (DNS), where an initial perturbed interface develops, in the presence of a parallel B_0, with elongated fingers separated by a distance $\lambda_c = 2\pi B_0^2/(\mathscr{A} g)$, which is somehow representative of the Crab nebula structure (Stone & Gardiner (2007*a*,*b*); Carlyle & Hillier (2017)).

The knowledge of this typical distance λ_c between structures and their growth rate α may be used to evaluate the intensity of the ambient magnetic field, under some strong hypothesis (Ryutova (2010); Hillier (2018)).

Note that in this configuration with a mean magnetic parallel to the interface, the interchange mode, such that $\boldsymbol{k} \cdot \boldsymbol{B}_0 = 0$, is not damped at all. This is the reason why magnetic shear has also been investigated (Carlyle & Hillier, 2017) where the direction of $\boldsymbol{B}_0$, still in the plane of the interface, is different in the lower and upper fluids.

In this work, we rather focus on the less investigated framwork where the mean magnetic field is perpendicular to the interface: this configuration remains statistically axisymetric. In this case, the growth rate of a single mode of wavelength $2\pi/k$ is damped, but the instability still occurs (Chandrasekhar (1961)): unlike the tangential magnetic field, there is no critical wavelength for which the instability is totally suppressed.

For a fully perturbed interface, Jun *et al.* (1995) observed with 2D simulations that, depending on the magnitude of B_0, the MRTI can be either enhanced or reduced with respect to the non-magnetic case. However, it is not clear how the 2D configuration affects the results: indeed, it is known that in the purely hydrodynamic case, 2D and 3D simulations of the RTI yield quite different results (Dimonte, 2004).

In order to shed some light on the MRTI, we propose to quantify how the vertical mean magnetic field affects mixing at small scales and the dynamics of large scales, thanks to high resolution DNS. In particular, we are interested in the transition between the early damped phase, where magnetic effects inhibit shear instabilities between structures and hence turbulent mixing, and a later regime where turbulence is strong enough to break the smooth elongated fingers.

EQUATIONS AND NUMERICAL SETUP

The motion of the two incompressible fluids, initially at rest in an unstable configuration and separated by a flat interface, is given by the following set of equations within the

Boussinesq approximation:

$$\left(\partial_t + \boldsymbol{u}\cdot\boldsymbol{\nabla} - \nu\nabla^2\right)\boldsymbol{u} = -\boldsymbol{\nabla} p - 2\mathscr{A} g C \boldsymbol{n}_3 + (\boldsymbol{\nabla}\times\boldsymbol{B})\times\boldsymbol{B}, \tag{1}$$

$$\left(\partial_t + \boldsymbol{u}\cdot\boldsymbol{\nabla} - \eta\nabla^2\right)\boldsymbol{B} = (\boldsymbol{B}\cdot\boldsymbol{\nabla})\boldsymbol{u}, \tag{2}$$

$$\left(\partial_t + \boldsymbol{u}\cdot\boldsymbol{\nabla} - \kappa\nabla^2\right)C = 0, \tag{3}$$

$$\boldsymbol{\nabla}\cdot\boldsymbol{u} = 0, \quad \boldsymbol{\nabla}\cdot\boldsymbol{B} = 0, \tag{4}$$

where $\boldsymbol{u}$ is the velocity field, $\boldsymbol{B}$ the total magnetic field scaled as a velocity, with $\boldsymbol{B} = \boldsymbol{b} + B_0\boldsymbol{n}_3$ and $\boldsymbol{n}_3$ the upward unit vector, C the concentration field, p is the reduced pressure, and ν, η and κ are respectively the kinematic viscosity, magnetic diffusivity and molecular diffusivity. For simplicity, we choose $\nu = \kappa = \eta$.

The pseudo-spectral code STRATOSPEC, previously used to investigate turbulent mixing within the Faraday instability (Briard *et al.* (2020)), is employed here to solve equations (1)-(4). The domain is a triply periodic cubic box of size 2π, and time advancement is realized using a third-order strong stability preserving Runge-Kutta scheme. To evaluate the effects of the magnitude of B_0, DNS with $N = 1024^3$ grid points are performed. A summary of the simulations is provided in Table 1.

Table 1. Parameters of the DNS: Number of points N, Atwood number times gravitational acceleration $\mathscr{A}g$, Mean vertical magnetic field intensity B_0, Diffusion coefficients ν.

Label	N	$\mathscr{A}g$	B_0	$\nu = \kappa = \eta$
R1B0	1024^3	0.5	0	2×10^{-4}
R1B01	1024^3	0.5	0.10	2×10^{-4}
R1B02	1024^3	0.5	0.20	2×10^{-4}
R1B05	1024^3	0.5	0.50	2×10^{-4}

At $t = 0$, only the scalar field is perturbed at the interface according to

$$C(\boldsymbol{x}, t=0) = \frac{1}{2}\left[1 + \tanh\left(\frac{z - \mathscr{S}(x,y)}{\sigma}\right)\right], \tag{5}$$

with $\sigma = 0.02$, a small parameter that ensures at least 20 points along z for the lowest resolution. $\mathscr{S}(x,y)$ is a deformation surface that is determined by a variance and a peak wavenumber: the same deformation is used for all simulations at a given resolution, with the peak wavenumber $40 \le k_p \le 50$, and an infrared slope like k^4.

With such an initialization, scalar perturbations induce velocity fluctuations through the buoyancy term $2\mathscr{A}gC$ in (1), which in turn produce magnetic fluctuations through the stretching term $B_0\partial_z\boldsymbol{u}$ in (2).

TRANSITION TO TURBULENT MIXING

First, in order to illustrate the impact of a vertical mean magnetic field on a developing mixing zone, the 3D concentration field C of DNS R1B0 is presented in figure 1 in the non-magnetic case. Shortly after $t = 0$, a variety of bubble-like structures appear. Merging and shearing between ascending and descending structures lead to turbulent mixing and a great diversity of scales, which can be deduced from the second image of figure 1 with intermediate values of C (light blue and yellow). Later on, the turbulent mixing zone $L(t)$ eventually grows like $L \sim t^2$ (Youngs, 1994).

If a vertical magnetic field is added to the previous configuration, the development of structures is dramatically altered, as revealed in figure 2. Indeed, instead of growing bubbles, the interface perturbations are stretched, without any mixing, which gives birth to these remarkable smooth fingers. The mean magnetic field inhibits small-scale shear instabilities between structures, which hence eventually grow faster than in the non magnetic case. When turbulence becomes strong enough to overcome the damping imposed by the magnetic field, fingers develop bubbles at their edges. Later on, the usual picture of a turbulent Rayleigh-Taylor mixing zone is recovered, with bubbles of different sizes, and complex interacting patches of scalar of different intensities, as can be seen on the sides of the DNS box in the third image of figure 2.

To better quantify the complex dynamics of the MRTI, we investigate in figure 3 the time evolution of the mixing zone size, defined as

$$L(t) = 6\int \langle C\rangle\left(1 - \langle C\rangle\right)\mathrm{d}z, \tag{6}$$

where $\langle\cdot\rangle$ refers to the horizontal average. At the instability onset, the non magnetic case (black) obviously increases the most rapidly, since there is no damping by the mean magnetic field. This is in agreement with the linear theory (Chandrasekhar, 1961) and with early 2D simulations by Jun *et al.* (1995). For $B_0 \neq 0$, the more intense B_0, the slower the growth of $L(t)$.

But later one, when turbulence becomes sufficiently intense to overcome the magnetic tension, structures break and one eventually recovers the usual picture of the RTI, with a nonlinear saturation that yields $L(t) = 2\alpha\mathscr{A}gt^2$, with α the growth rate of the "bubbles", which is approximately $\alpha = 0.02$ in R1B0.

It is possible to be more specific about the statement that structures break when "turbulence becomes strong enough". In fact, such a criterion was already invoked in Jun *et al.* (1995). Considering the (vertical) interface between ascending and descending smooth structures in the case of a sufficiently intense vertical B_0, this amounts to a kind of magnetic Kelvin-Helmholtz configuration, without any gravity. The inviscid linear stability analysis of the magnetic Kelvin-Helmholtz flow was performed in Chandrasekhar (1961), and in the present situation this eventually yields that the structures are destabilized if

$$V_3 > B_0, \tag{7}$$

namely if the typical turbulent vertical velocity V_3 exceeds the Alfvèn velocity B_0. To verify this criterion, we choose $V_3 = \sqrt{\overline{u_3^2}}$, where $\overline{u_3^2}$ is the vertical kinetic energy. The comparison between the DNS results and the simple criterion (7) is presented in figure 4.

The ratio V_3/B_0 is presented for three different values of B_0. For the lowest value $B_0 = 0.10$, V_3 overcomes B_0 quite early, and a change of regime is observed around $t \simeq 3$, which was already seen in figure 3. This change of dynamics illus-

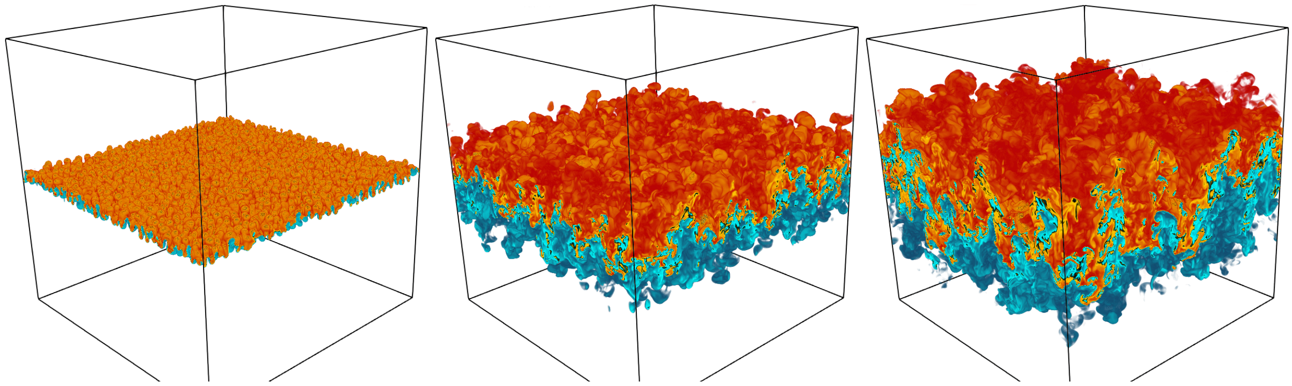

Figure 1. Time evolution of the concentration field C (from left to right) of DNS R1B0 1024^3, without any magnetic field. The color scale indicates the value of C, that varies between 0 (dark blue) and 1 (red); pure fluids are transparent.

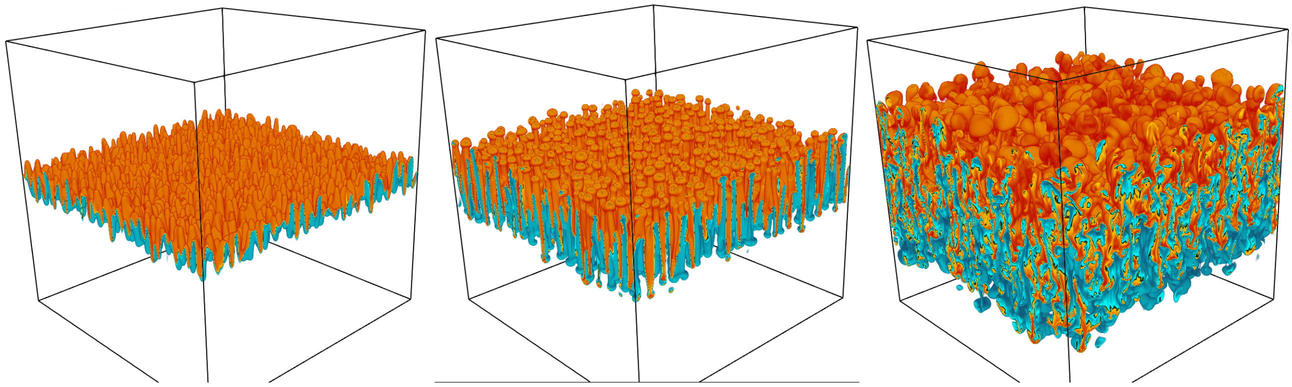

Figure 2. Time evolution of the concentration field C (from left to right) of DNS R1B02 1024^3, with the vertical mean magnetic field intensity $B_0 = 0.2$. The color map is the same as figure 1.

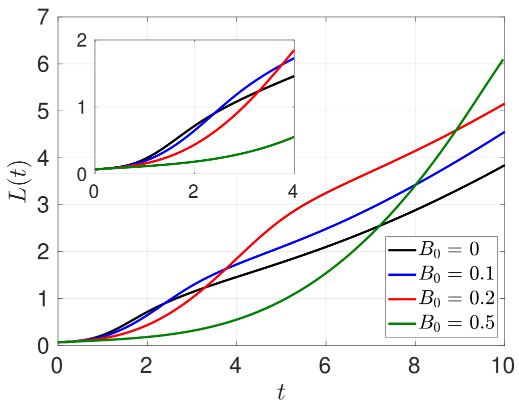

Figure 3. Effects of the mean magnetic field intensity B_0 in the R1 simulations. Mixing zone size L (6).

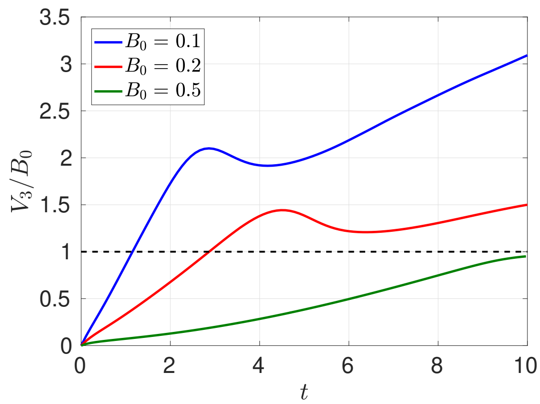

Figure 4. Effects of the mean magnetic field intensity B_0 in the R1 simulations. Normalized vertical velocity with the Alfven velocity V_3/B_0, see criterion (7).

trates the transition between smooth growing fingers, and turbulent mixing of sheared bubbles: this will be better characterized in terms of anisotropy and mixing later on.

For $B_0 = 0.20$, the transition happens later since the magnetic damping is stronger. Finally, for the strongest Alfvèn velocity $B_0 = 0.5$, turbulence is never intense enough to overcome the mean magnetic field and generate small-scale shear instabilities between structures. Hence, the criterion (7), originating from inviscid linear stability analysis, provides a lower bound for the transition to turbulence in the MRTI.

Now that we have shown that transition to turbulence corresponds to a slowing down of the turbulent mixing zone growth, which is well characterized by the ratio of the vertical turbulent velocity and Alfvèn velocity, we turn our attention to mixing, and define the so-called mixing parameter

$$\Theta = 1 - \frac{6}{L} \int \langle c^2 \rangle \mathrm{d}z, \tag{8}$$

where $\langle c^2 \rangle$ refers to the horizontal average of the concentration variance. This mixing parameter quantifies how well the two fluids are mixed together, with $\Theta = 1$ for perfectly mixed

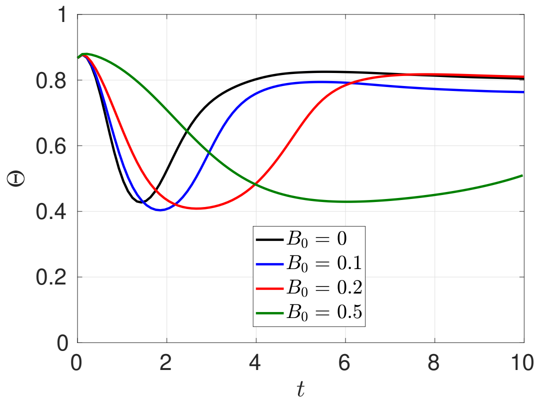

Figure 5. Effects of the mean magnetic field intensity B_0 in the R1 simulations. Mixing parameter Θ defined in (8).

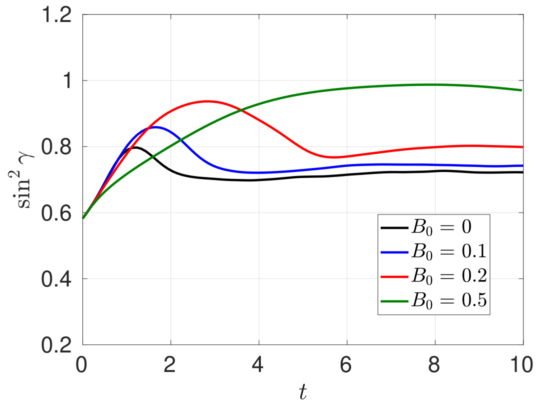

Figure 6. Effects of the mean magnetic field intensity B_0 in the R1 simulations. Global anisotropy parameter $\sin^2\gamma$ defined in (9).

fluids. In classical RTI, this parameter can be related to the growth rate α of the mixing zone under the Boussinesq approximation (Gréa (2013)).

We investigate in figure 5 this mixing parameter for different values of the mean vertical magnetic field B_0. For the non magnetic case, Θ tends to 0.8 after a transient regime, value which is typical for the RTI (see fig9 in Gréa (2013) and references therein). For a weak magnetic field $B_0 = 0.10$, the transient regime is longer, but the final state remains close to the hydrodynamic case. Nevertheless, the final value of Θ is slightly smaller, showing that the initial damping of the mean magnetic field is reflected in the long-time dynamics.

More interestingly, this behavior is not monotonous with increasing B_0. Indeed, when the mean magnetic field intensity is further increased to $B_0 = 0.20$, the transient regime is once again longer, but the final value of Θ is the same as in the non-magnetic case. Therefore, according to these global quantities, it seems that there is an optimal B_0 for a given configuration that boosts turbulence: this observation was already made in 2D simulations (Jun *et al.*, 1995).

Finally, for $B_0 = 0.50$, as already seen in figure 4, there is never a transition to turbulence, so that magnetic tension always inhibits small-scale shearing instabilities, and no mixing occurs. Remark that the strong initial decrease of Θ reflects the length of the transient regime where structures grow without significant small-scale shear. For different initial conditions, with bigger perturbations for instance, the initial value of Θ could be smaller.

Finally, we analyze the anisotropy at the level of the scalar field. This is done thanks to the following parameter

$$\sin^2\gamma = \frac{\int_0^\infty \int_0^\pi \mathscr{E}_{cc}(\boldsymbol{k}) \sin^3\theta \mathrm{d}\theta \mathrm{d}k}{\int_0^\infty \int_0^\pi \mathscr{E}_{cc}(\boldsymbol{k}) \sin\theta \mathrm{d}\theta \mathrm{d}k}, \tag{9}$$

where $\mathscr{E}_{cc}(\boldsymbol{k}) = \hat{c}(\boldsymbol{k})\hat{c}(\boldsymbol{k})$ is the spectral variance density, $\hat{c}$ is the Fourier transform of the concentration fluctuation $c = C - \langle C \rangle$, so that $\iint k^2 \mathscr{E}_{cc} \sin\theta \mathrm{d}\theta \mathrm{d}k = \overline{c^2}$, with $\boldsymbol{k} \cdot \boldsymbol{n}_3 = k\cos\theta$. In particular, for an isotropic field, $\sin^2\gamma = 2/3$.

This global anisotropy parameter is presented in figure 6. Remarks comparable to those regarding Θ can be made, namely that the stronger B_0, the longer the transient regime. In this transient regime, $\sin^2\gamma$ first increases, which reflects the stretching of the initial interface perturbations under the effects of gravity. The mean magnetic field amplifies this anisotropy by stretching even more the structures. Note that values like $2/3 \leq \sin^2\gamma \leq 1$ correspond to vertically elongated structures.

When there is an effective transition to turbulence with small-scale shear instabilities, $\sin^2\gamma$ is significantly reduced, which is correlated to the increase of Θ in figure 5, due to the return to isotropy of the smallest scales of the flow. Except for $B_0 = 0.5$, where the Alfvèn velocity is so strong that the smooth elongated fingers continue to grow without mixing.

An interesting feature here, different from the observations made regarding Θ, is that even in the asymptotic state, the final value of $\sin^2\gamma$ increases with B_0, which shows that there is still a strong imprint, in the fully turbulent regime, of the vertical anisotropy imposed by the mean magnetic field.

CONCLUSIONS

The Rayleigh-Taylor instability submitted to a mean vertical magnetic field has been investigated with the use of high resolution DNS. The dramatic effect of the Lorentz force on the overall dynamics is to initially inhibit small-scale shear instabilities between ascending and descending structures, so that mixing is strongly damped. Instead of turbulent bubbles, smooth elongated fingers emerge, that grow rapidly since there is no small scale mixing.

When turbulence becomes strong enough, meaning that the typical vertical velocity of the fluid exceeds the Alfvèn velocity, shear eventually induces mixing, fingers break and traditional bubbles are recovered. The mixing and global anisotropy parameters were investigated to better quantify this transition to turbulence, and the outcome is interesting. It seems that there is an optimal value of B_0 such that mixing remains as effective as the non-magnetic case. This is possibly because with a long transient where smooth elongated fingers grow, a larger surface for mixing becomes available when the flow transitions to turbulence.

Regarding anisotropy, the conclusion is somehow different, since even in the fully turbulent regime, the vertical anisotropy of the concentration field is greater for larger B_0, which is a permanent imprint of the mean vertical magnetic field.

The perspectives of this study are to investigate more deeply two-point statistics in order to provide scale-by-scale information about anisotropy, but also spectral scalings. We wish also to perform simulations at better resolution to increase the level of turbulence, and investigate if the observations made regarding the "booster effect" of the vertical mean magnetic field persist.

REFERENCES

Briard, A., Gostiaux, L. & Gréa, B.-J. 2020 The turbulent Faraday instability in miscible fluids. *Journal of Fluid Mechanics* **883**, A57.

Carlyle, J. & Hillier, A. 2017 The non-linear growth of the magnetic Rayleigh-Taylor instability. *Astronomy & Astrophysics* **605**, A101.

Chandrasekhar, S. 1961 X: The stability of superimposed fluids: the Rayleigh-Taylor instability. In *Hydrodynamic and Hydromagnetic Stability*, pp. 428–477. Oxford University Press.

Dimonte, G. et al. 2004 A comparative study of the turbulent Rayleigh-Taylor instability using high-resolution three-dimensional numerical simulations: The Alpha-Group collaboration. *Physics of Fluids* **16**, 1668.

Gréa, B.-J. 2013 The rapid acceleration model and the growth rate of a turbulent mixing zone induced by Rayleigh-Taylor instability. *Physics of Fluids* **25**, 015118.

Hillier, A. 2018 The magnetic Rayleigh-Taylor instability in solar prominences. *Rev. Mod. Plasma Phys.* **2**, 1–47.

Jun, B.-I., Norman, M.L. & Stone, J.M. 1995 The non-linear growth of the magnetic Rayleigh-Taylor instability. *The Astrophysical Journal* **453**, 332–349.

Ryutova, M. et al. 2010 Observation of plasma instabilities in quiescent prominences. *Solar Phys.* **267**, 75–94.

Stone, J.M. & Gardiner, T. 2007*a* The magnetic Rayleigh-Taylor instability in three dimensions. *The Astrophysical Journal* **671**, 1726–1735.

Stone, J.M. & Gardiner, T. 2007*b* Nonlinear evolution of the magnetohydrodynamic Rayleigh-Taylor instability. *Physics of Fluids* **19**, 094104.

Youngs, D.L. 1994 Numerical simulation of mixing by Rrayleigh-Taylor and Richtmyer-Meshkov instabilities. *Laser Particle Beams* **12**, 725–750.